Supporting Information

Zero-Dimensional Organic-Inorganic Perovskite Variant: Transition between Molecular and Solid Crystal

Ming-Gang Ju,[1] Jun Dai,[1] Liang Ma,[1] Yuanyuan Zhou,[2] Xiao Cheng Zeng[1,3*]

[1]Department of Chemistry and Nebraska Center for Materials and Nanoscience, University of Nebraska-Lincoln, Lincoln, Nebraska, 68588, United States

[2]School of Engineering, Brown University, Providence, Rhode Island 02912, United States

[3]Department of Chemical & Biomolecular Engineering and Department of Mechanical & Materials Engineering, University of Nebraska-Lincoln, Lincoln, Nebraska, 68588, United States

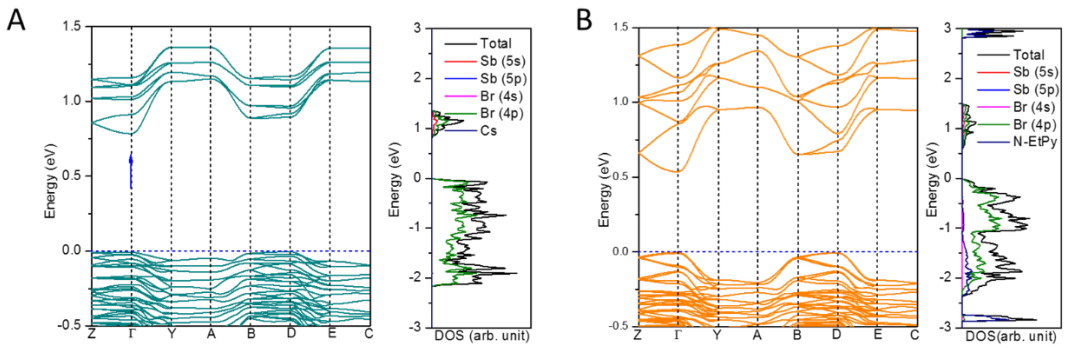

Figure S1. Computed band structure and DOS of $CsSbBr_6$ (A) and N-EtPy$SbBr_6$ (B) using PBE functional, Γ (0.0, 0.0, 0.0), Z (0.0, 0.0, 0.5), Y (0.0, 0.5, 0.0), A (-0.5, 0.5, 0.0), B (-0.5, 0.0, 0.0), D (-0.5, 0.0, 0.5), E (-0.5, 0.5, 0.5) and C (0.0, 0.5, 0.5) refer to the high-symmetry special points in the first Brillouin zone.

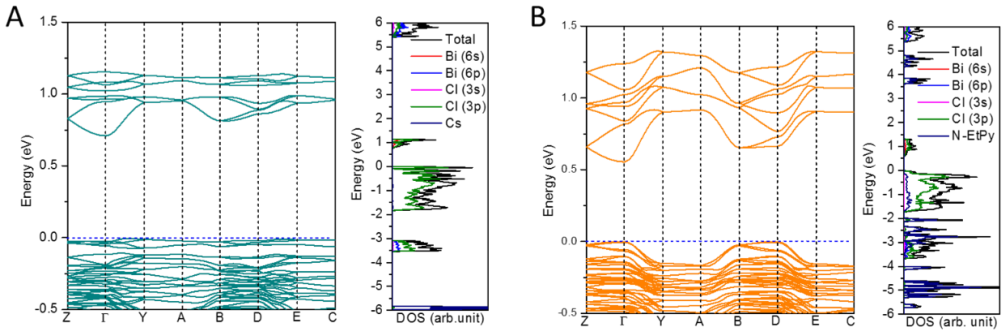

Figure S2. Computed band structure and DOS of $CsBiCl_6$ (A) and N-EtPy$BiCl_6$ (B) using PBE functional, Γ (0.0, 0.0, 0.0), Z (0.0, 0.0, 0.5), Y (0.0, 0.5, 0.0), A (-0.5, 0.5, 0.0), B (-0.5, 0.0, 0.0), D (-0.5, 0.0, 0.5), E (-0.5, 0.5, 0.5) and C (0.0, 0.5, 0.5) refer to the high-symmetry special points in the first Brillouin zone.

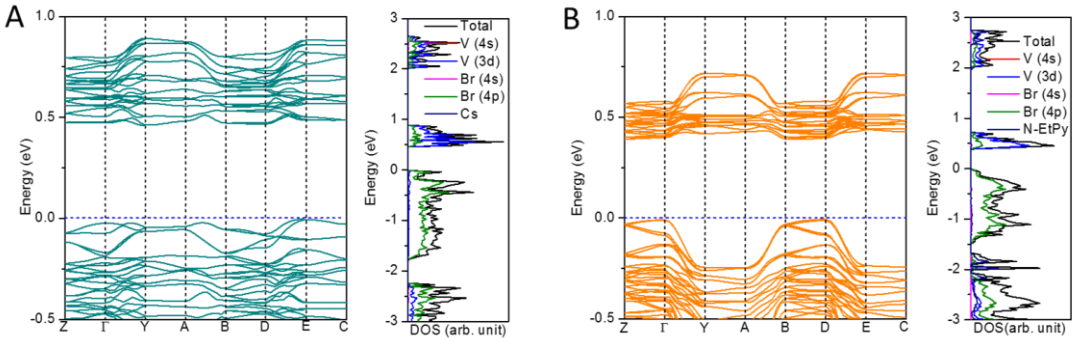

Figure S3. Computed band structure and DOS of $CsVBr_6$ (A) and N-EtPyVBr_6 (B) using PBE functional, Γ (0.0, 0.0, 0.0), Z (0.0, 0.0, 0.5), Y (0.0, 0.5, 0.0), A (-0.5, 0.5, 0.0), B (-0.5, 0.0, 0.0), D (-0.5, 0.0, 0.5), E (-0.5, 0.5, 0.5) and C (0.0, 0.5, 0.5) refer to the high-symmetry special points in the first Brillouin zone.

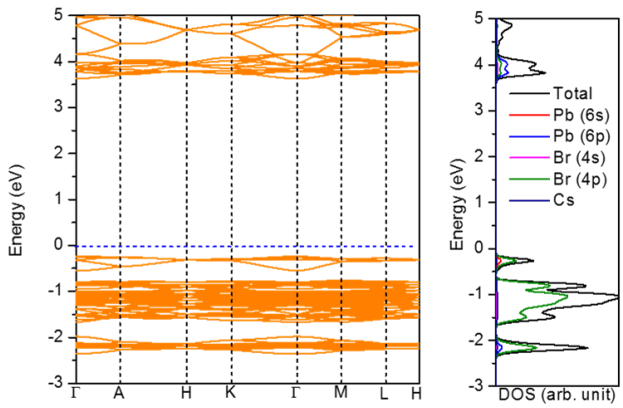

Figure S4. Computed band structure and DOS of Cs_4PbBr_6 using PBE functional, Γ (0.0, 0.0, 0.0), A (0.0, 0.0, 0.5), H (-0.3333, 0.6667, 0.0), K (-0.3333, 0.6667, 0.0), M (0.0, 0.5, 0.0) and L (0.0, 0.5, 0.5) refer to the high-symmetry special points in the first Brillouin zone.

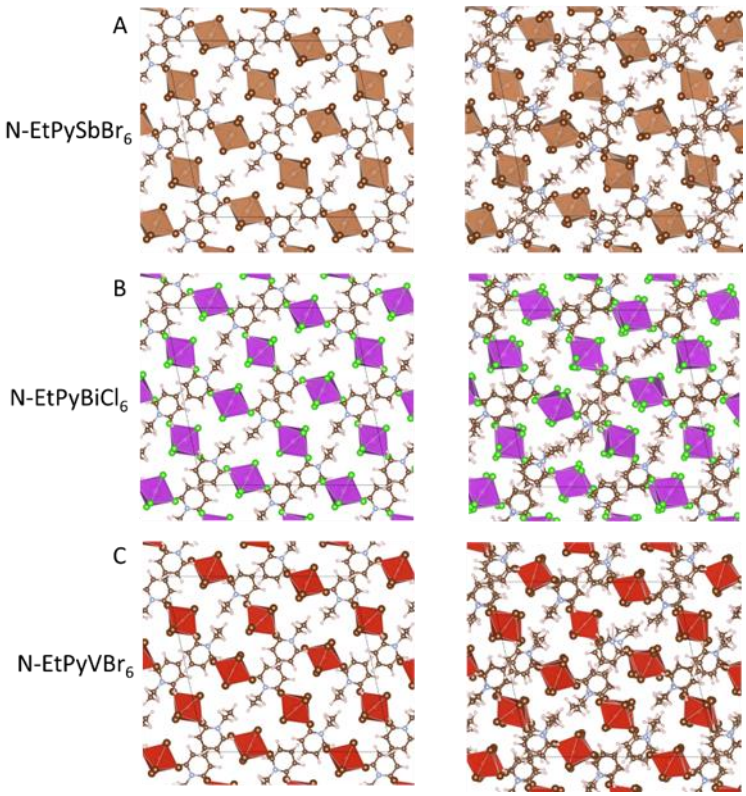

Figure S5. Snapshots of N-EtPySbBr6, N-EtPyBiCl6 and N-EtPyVBr6 at initial (left) and 5 ps (right) from AIMD simulation with temperature controlled at 300 K (*NVT* ensemble).

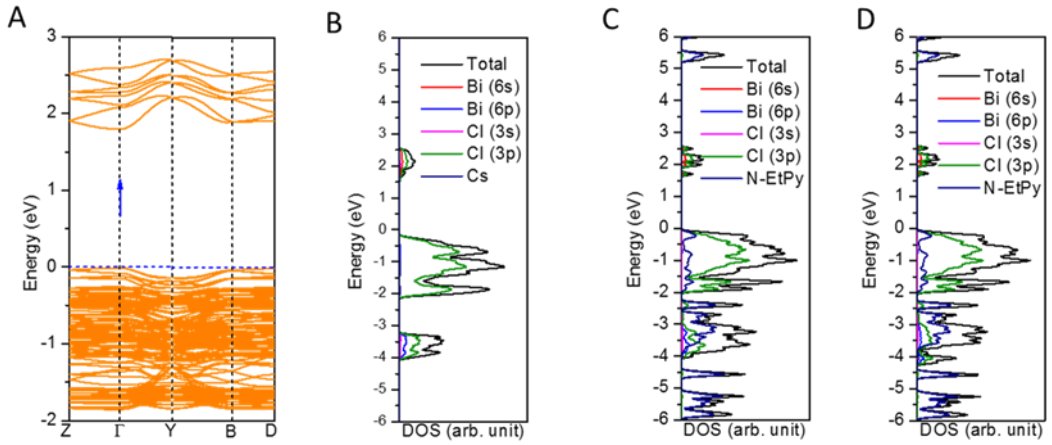

Figure S6. Computed band structure (A) and DOS (B) of N-EtPyBiCl$_6$ using HSE06 functional, Γ (0.0, 0.0, 0.0), Z (0.0, 0.0, 0.5), Y (0.0, 0.5, 0.0), B (-0.5, 0.0, 0.0) and D (-0.5, 0.0, 0.5) refer to the high-symmetry special points in the first Brillouin zone. Computed DOSs of N-EtPyBiCl$_6$ using HSE06 functional without (C) and with (D) SOC (with only the Γ point).

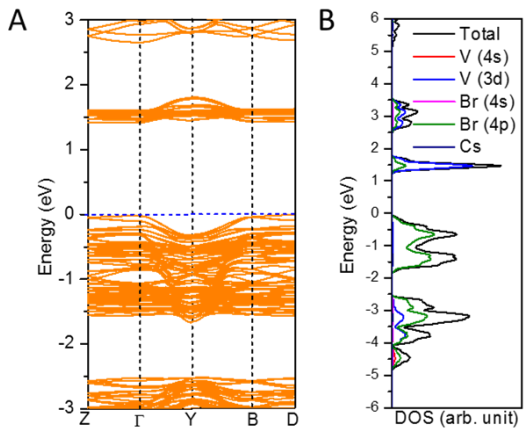

Figure S7. Computed band structure (A) and DOS (B) of N-EtPyVBr$_6$ using HSE06 functional, Γ (0.0, 0.0, 0.0), Z (0.0, 0.0, 0.5), Y (0.0, 0.5, 0.0), B (-0.5, 0.0, 0.0) and D (-0.5, 0.0, 0.5) refer to the high-symmetry special points in the first Brillouin zone.

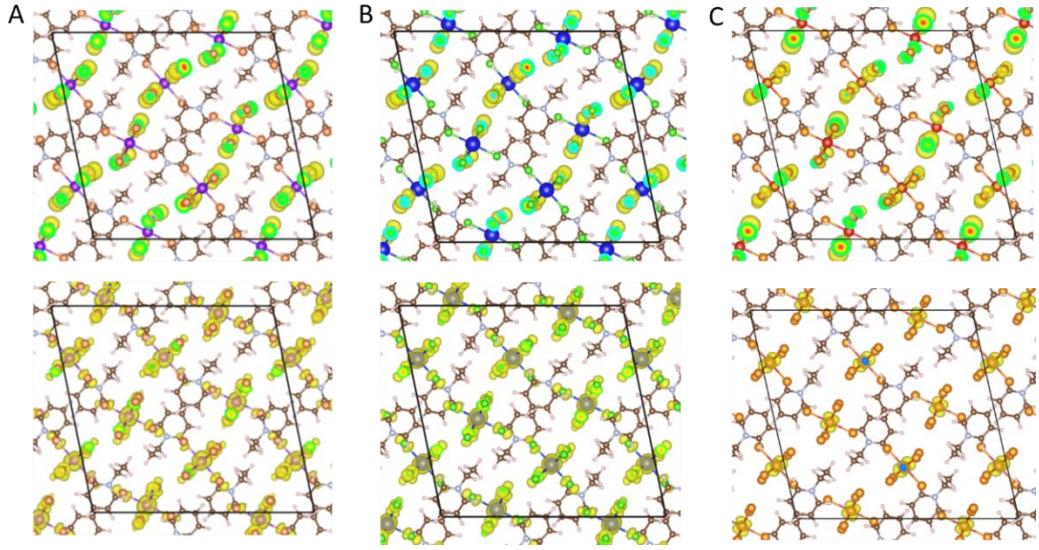

Figure S8. Computed charge density distribution of the highest VB and lowest CB of a periodic slab model of N-EtPySbBr$_6$, N-EtPyBiCl$_6$ and N-EtPyVBr$_6$ based on the PBE functional.

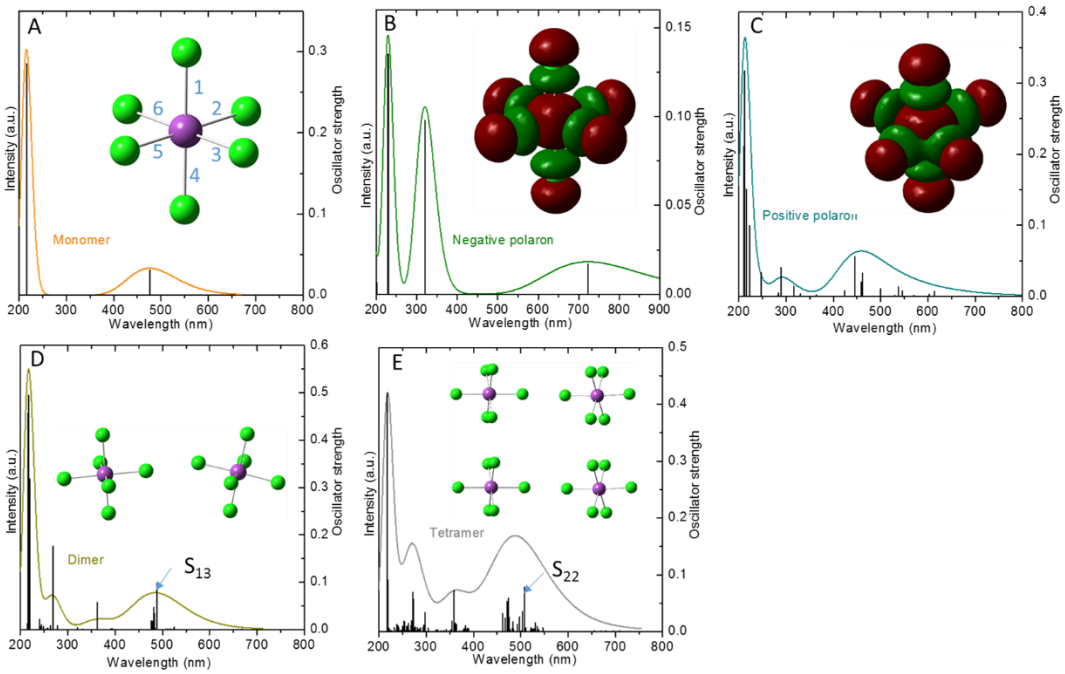

Figure S9. (A) Absorption spectrum of monomer of $[BiCl_6]^{-1}$ with neutral state. The configuration is given in inset. (B) Absorption spectrum of monomer with negative polaron state. The spin distribution of negative polaron is given in inset. (C) Absorption spectrum of monomer with positive polaron state. The spin distribution of positive polaron is given in inset. (D) Absorption spectrum of dimers with neutral state. (E) Absorption spectrum of tetramers with neutral state.

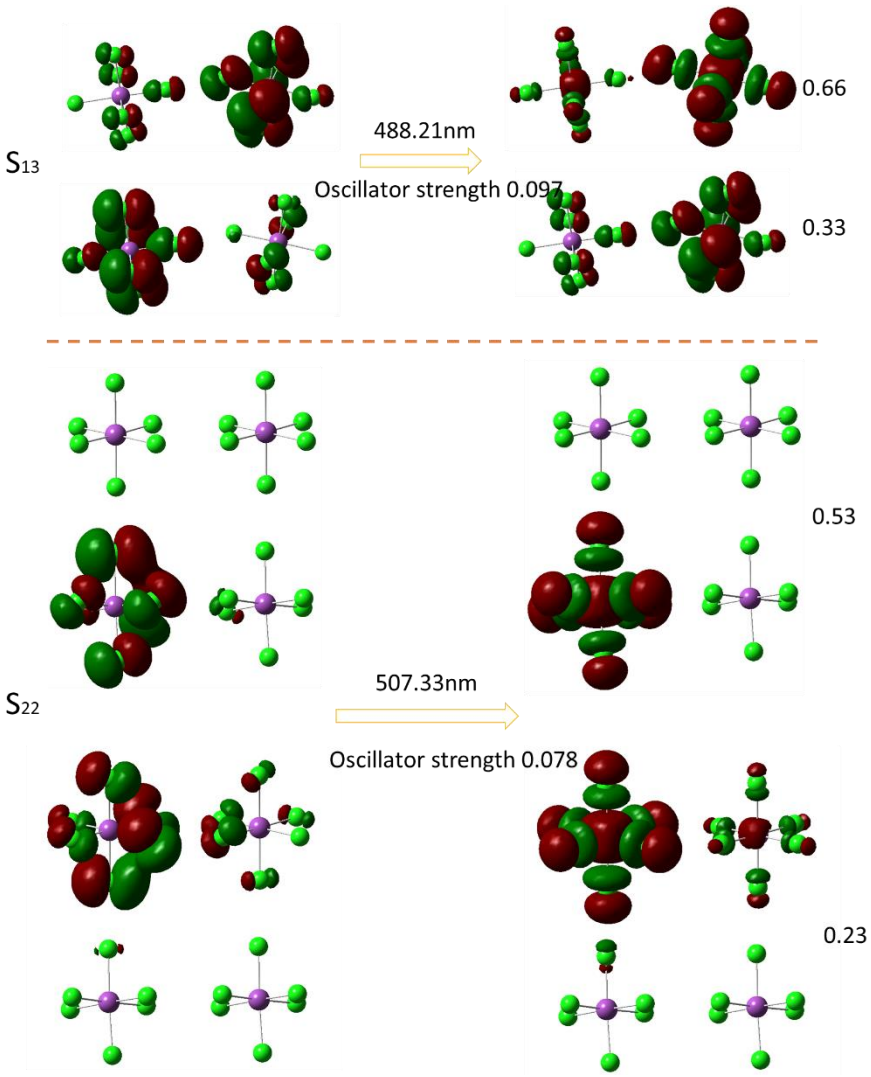

Figure S10. Computed electronic densities of "hole" (right) and "particle" (left) NTO pairs for the dipole-allowed singlet excited states of dimer (A) and tetramers (B) of $[BiCl_6]^{-1}$.

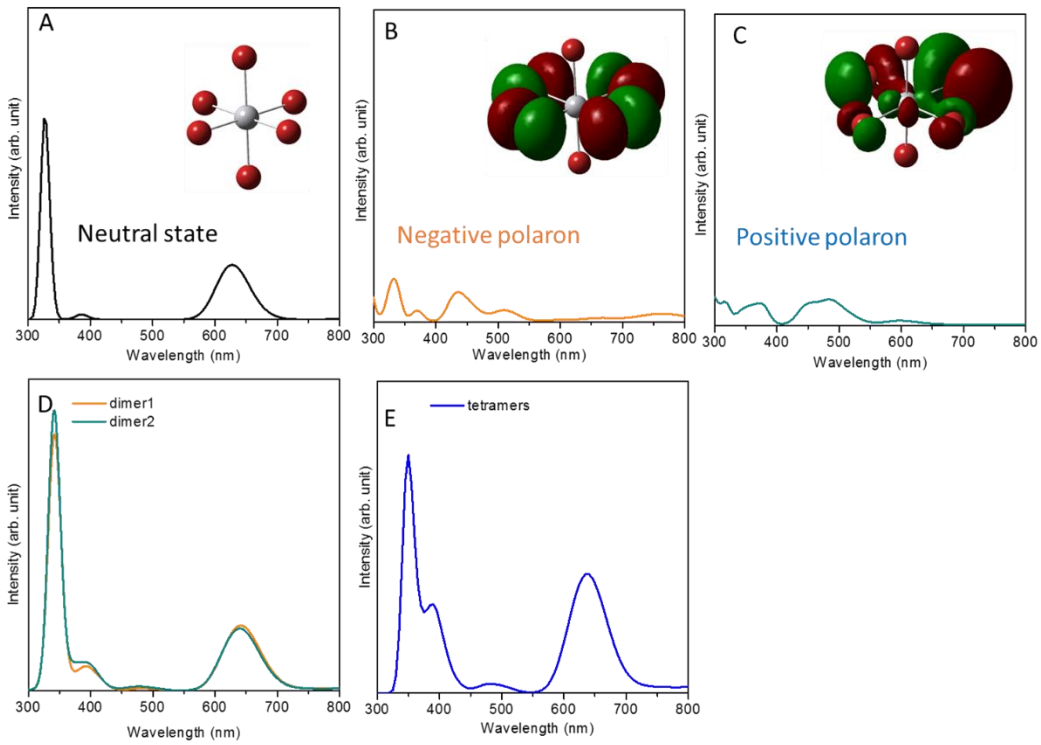

Figure S11. (A) Absorption spectrum of monomer of $[VBr_6]^{-1}$ with neutral state. The configuration is given in inset. (B) Absorption spectrum of monomer with negative polaron state. The spin distribution of negative polaron is given in inset. (C) Absorption spectrum of monomer with positive polaron state. The spin distribution of positive polaron is given in inset. (D) Absorption spectrum of dimers with neutral state. (E) Absorption spectrum of tetramers with neutral state.

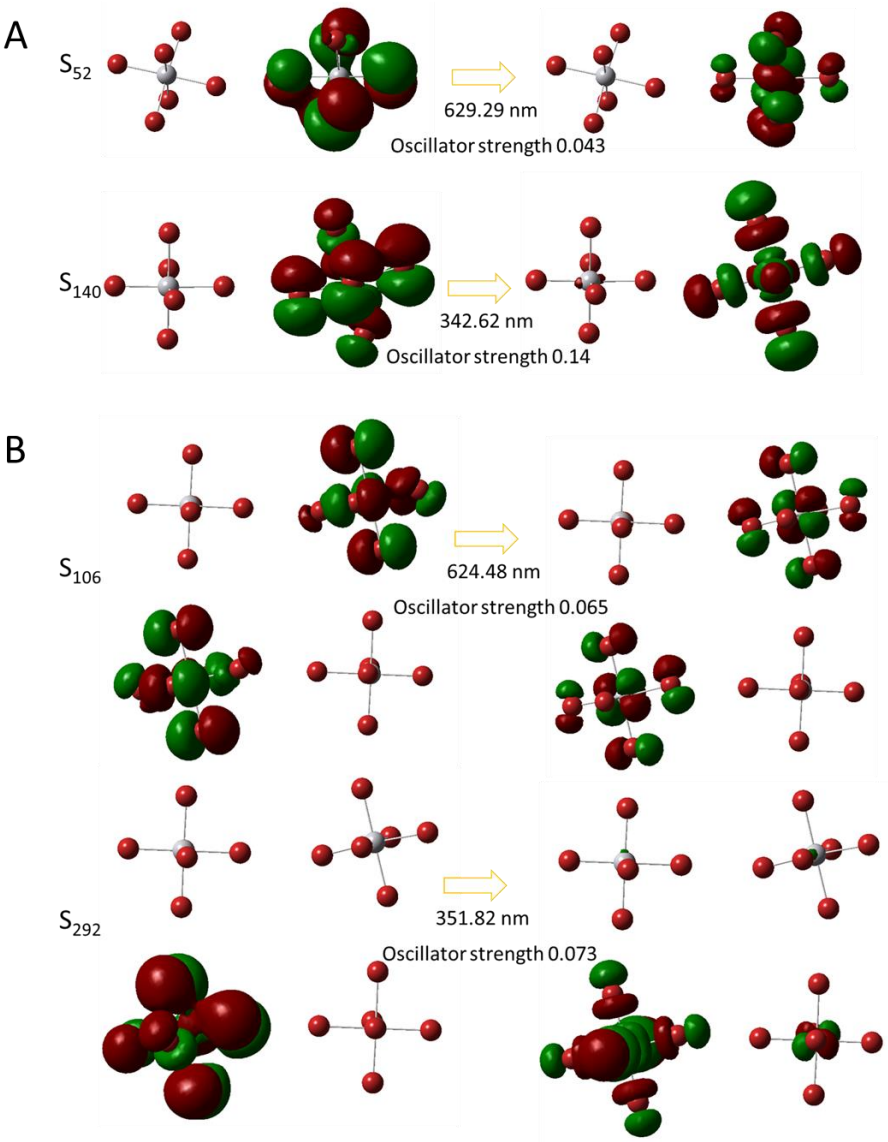

Figure S12. Computed electronic densities of "hole" (right) and "particle" (left) NTO pairs for the dipole-allowed singlet excited states of dimer (A) and tetramers (B) of $[VBr_6]^{-1}$.

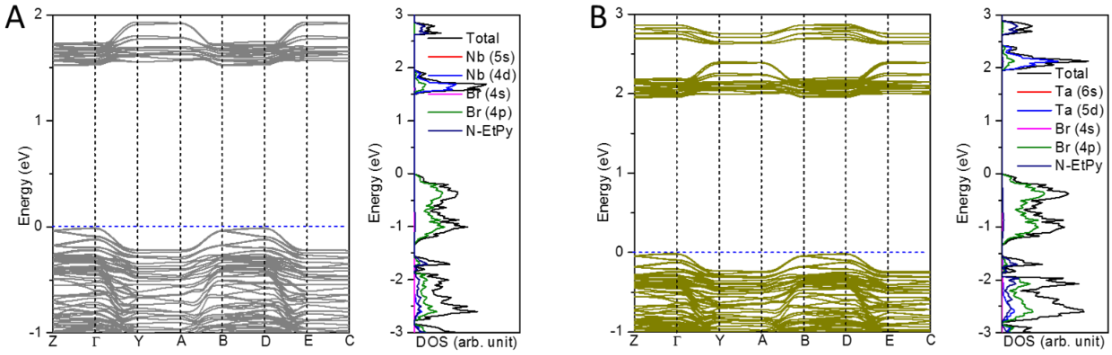

Figure S13. Computed band structure and DOS of N-EtPyNbBr$_6$ (A) and N-EtPyTaBr$_6$ (B) using PBE functional, Γ (0.0, 0.0, 0.0), Z (0.0, 0.0, 0.5), Y (0.0, 0.5, 0.0), A (-0.5, 0.5, 0.0), B (-0.5, 0.0, 0.0), D (-0.5, 0.0, 0.5), E (-0.5, 0.5, 0.5) and C (0.0, 0.5, 0.5) refer to the high-symmetry special points in the first Brillouin zone.

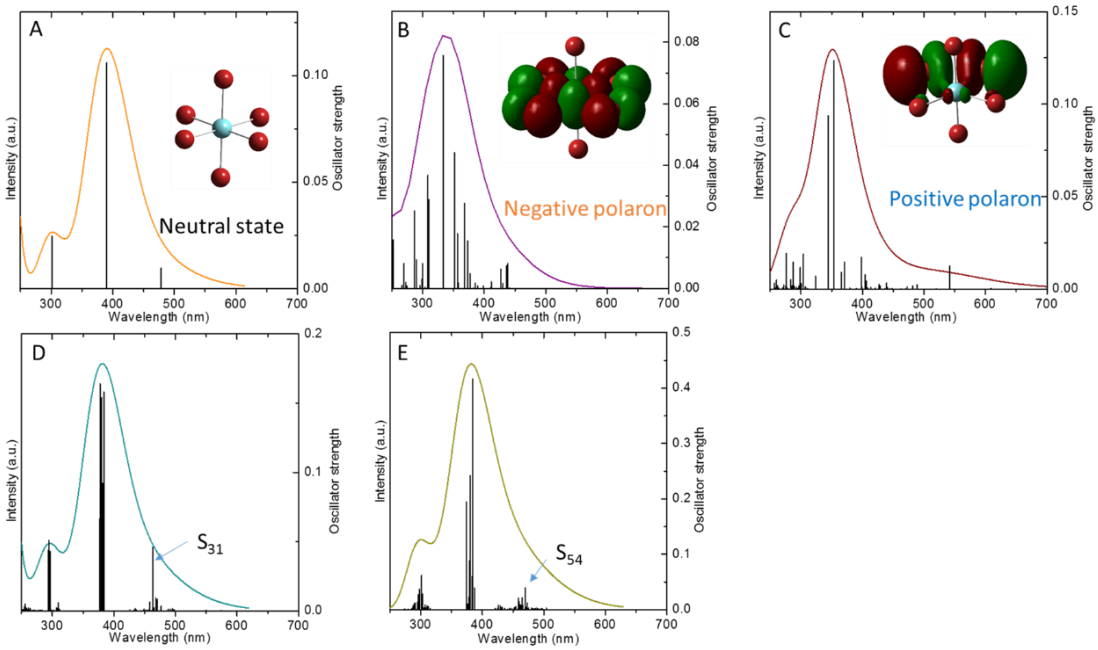

Figure S14. (A) Absorption spectrum of monomer of $[NbBr_6]^{-1}$ with neutral state. The configuration is given in inset. (B) Absorption spectrum of monomer with negative polaron state. The spin distribution of negative polaron is given in inset. (C) Absorption spectrum of monomer with positive polaron state. The spin distribution of positive polaron is given in inset. (D) Absorption spectrum of dimers with neutral state. (E) Absorption spectrum of tetramers with neutral state.

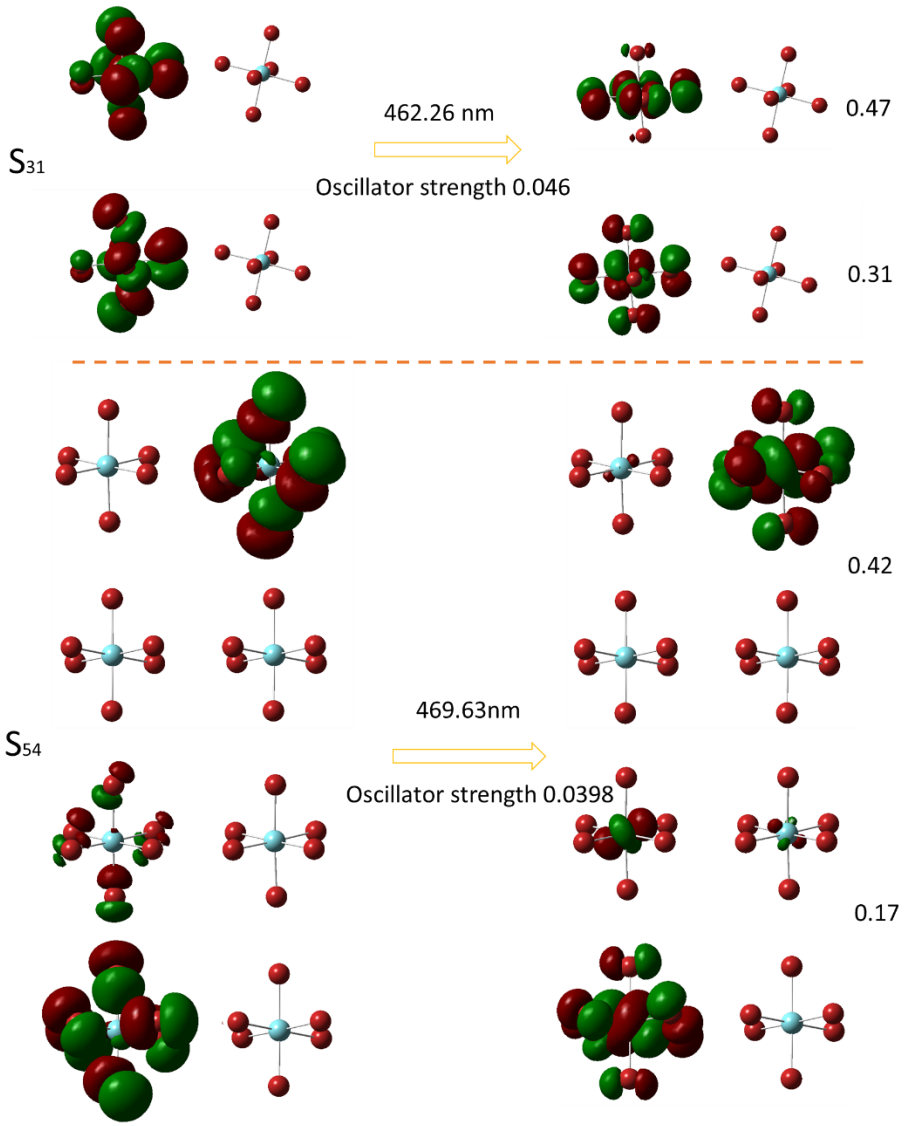

Figure S15. Computed electronic densities of "hole" (right) and "particle" (left) NTO pairs for the dipole-allowed singlet excited states of dimer (A) and tetramers (B) of $[NbBr_6]^{-1}$.

TABLE S1. Optimized bond lengths of Sb-Br, Bi-Cl, V-Br, Nb-Br and Ta-Br for monomer with different charge. (Å)

		1	2	3	4	5	6
Sb-Br	Neutral	2.59	2.59	2.59	2.59	2.59	2.59
	Positive	2.53	2.76	2.50	2.53	2.50	2.76
	Negative	2.74	2.74	2.74	2.74	2.74	2.74
Bi-Cl	Neutral	2.52	2.52	2.52	2.52	2.52	2.52
	Positive	2.46	2.70	2.43	2.46	2.43	2.70
	Negative	2.67	2.67	2.67	2.67	2.67	2.67
V-Br	Neutral	2.41	2.41	2.41	2.41	2.41	2.41
	Positive	2.32	2.69	2.26	2.32	2.26	2.69
	Negative	2.46	2.51	2.51	2.46	2.51	2.50
Nb-Br	Neutral	2.56	2.56	2.56	2.56	2.56	2.56
	Positive	2.49	2.77	2.44	2.49	2.44	2.77
	Negative	2.65	2.63	2.63	2.65	2.63	2.63
Ta-Br	Neutral	2.55	2.55	2.55	2.55	2.55	2.55
	Positive	2.48	2.73	2.43	2.48	2.43	2.73
	Negative	2.62	2.63	2.63	2.62	2.63	2.63

TABLE S2. Calculated charge transfer parameters and mobility of the N-EtPySbBr$_6$.

	channel	$V_{h/e}$ (meV)	d (Å)	k_i (s^{-1})	D (cm^2/s)	μ ($cm^2V^{-1}s^{-1}$)
electron	1	142.6	8.43	1.20×10^{10}	2.00×10^{-5}	7.73×10^{-4}
	2	94.8	7.38	5.32×10^{9}		
	3	53.3	7.36	1.68×10^{9}		
	4	170.4	8.35	1.72×10^{10}		
	5	0.278	7.66	4.57×10^{4}		
	6	36.6	7.97	7.93×10^{8}		
hole	1	0.02	8.43	1.87	9.48×10^{-9}	3.67×10^{-7}
	2	41.10	7.38	6.51×10^{6}		
	3	0.50	7.36	9.53×10^{2}		
	4	23.4	8.35	2.11×10^{6}		
	5	0.26	7.66	2.56×10^{2}		
	6	3.19	7.97	3.93×10^{4}		

TABLE S3. Calculated charge transfer parameters and mobility of the N-EtPyBiCl$_6$.

	channel	$V_{h/e}$ (meV)	d (Å)	k_i (s^{-1})	D (cm^2/s)	μ ($cm^2V^{-1}s^{-1}$)
electron	1	99.8	8.02	8.14×10^{9}	1.54×10^{-5}	5.94×10^{-4}
	2	79.8	7.13	5.20×10^{9}		
	3	144.3	8.10	1.70×10^{10}		
	4	43.3	7.05	1.53×10^{9}		
	5	35.9	7.70	1.06×10^{9}		
	6	7.5	7.42	4.53×10^{7}		
hole	1	0.24	8.02	1.47×10^{2}	5.41×10^{-9}	2.09×10^{-7}
	2	34.6	7.13	3.20×10^{6}		
	3	0.47	8.10	5.89×10^{2}		
	4	1.86	7.05	9.26×10^{3}		
	5	0.77	7.70	1.58×10^{3}		
	6	1.05	7.42	2.94×10^{3}		

TABLE S4. Calculated electronic couplings of the N-EtPyVBr$_6$, N-EtPyNbBr$_6$ and N-EtPyTaBr$_6$.

		N-EtPyVBr$_6$	N-EtPyNbBr$_6$	N-EtPyTaBr$_6$
	channel	$V_{h/e}$ (meV)	$V_{h/e}$ (meV)	$V_{h/e}$ (meV)
electron	1	0.013	7.12	8.12
	2	0.021	1.48	1.87
	3	0.091	0.57	1.75
	4	0.123	3.46	3.56
	5	0.091	2.77	1.23
	6	0.048	4.59	0.32
hole	1	0.001	2.13	0.23
	2	0.002	0.20	104.71
	3	0.002	6.86	0.92
	4	0	6.93	0.01
	5	0	29.55	7.43
	6	0	0.098	6.6